Exceptional Points in the Baxter-Fendley Free Parafermion Model

Robert A. Henry* and Murray T. Batchelor[†]

Mathematical Sciences Institute, The Australian National University, Canberra ACT
2601, Australia
* robert.henry@anu.edu.au
[†] murray.batchelor@anu.edu.au

January 30, 2023

Abstract

Certain spin chains, such as the quantum Ising chain, have free fermion spectra
which can be expressed as the sum of decoupled two-level fermionic systems.
Free parafermions are a simple generalisation of this idea to $\mathbb{Z}_N$-symmetric
models. In 1989 Baxter discovered a non-Hermitian but $\mathcal{PT}$-symmetric model
directly generalising the Ising chain which was much later recognised by Fendley to be a free parafermion spectrum. By extending the model's magnetic
field parameter to the complex plane, we show that a series of exceptional
points emerges, where the quasienergies defining the free spectrum become
degenerate. An analytic expression for the locations of these points is derived,
and various numerical investigations are performed. These exceptional points
also exist in the Ising chain with a complex transverse field. Although the
model is not in general $\mathcal{PT}$-symmetric at these exceptional points, their proximity can have a profound impact on the model on the $\mathcal{PT}$-symmetric real
line. Furthermore, in certain cases an exceptional point may appear on the
real line (with negative field).

1 Introduction

The $\mathbb{Z}_N$-symmetric free parafermion model is a quantum spin chain where the sites are "clocks" with N symmetric states. On a chain of length L with open boundary conditions it has the Hamiltonian

$$H = -\sum_{j=1}^{L-1} Z_j^\dagger Z_{j+1} - \lambda \sum_{j=1}^{L} X_j, \tag{1}$$

where X and Z are generalisations of the Pauli matrices given by

$$Z = \begin{pmatrix} 1 & 0 & 0 & \dots & 0 \\ 0 & \omega & 0 & \dots & 0 \\ 0 & 0 & \omega^2 & \dots & 0 \\ \vdots & \vdots & \vdots & \ddots & \vdots \\ 0 & 0 & 0 & \dots & \omega^{N-1} \end{pmatrix}, \quad X = \begin{pmatrix} 0 & 0 & 0 & \dots & 0 & 1 \\ 1 & 0 & 0 & \dots & 0 & 0 \\ 0 & 1 & 0 & \dots & 0 & 0 \\ \vdots & \vdots & \vdots & \ddots & \vdots & \vdots \\ 0 & 0 & 0 & \dots & 1 & 0 \end{pmatrix}. \tag{2}$$

The parameter λ is a constant assumed to be real and positive in the literature, and $\omega = e^{2\pi i/N}$ is an Nth root of unity.

When $N = 2$, the model reduces to the widely studied transverse field Ising model, with X and Z reducing to the Pauli matrices σ^x and σ^z. For $N > 2$, the model is non-Hermitian and has a complex spectrum. Importantly, the spectrum is known exactly for all N, L and λ, taking the form of *free parafermions*. This form was first observed by Baxter, who also formulated the model [1, 2], and later proved by Fendley using the Fradkin-Kadanoff transformation [3]. This solution was further explored and extended to the related classical model by Baxter [4], and Au-Yang and Perk [5,6]. This classical model is the τ_2 model, which is essential to the solution of the chiral Potts model [7]. In his solution, Fendley developed interesting algebraic techniques which were also applied to multispin free fermion systems [8]. This approach was later adopted and generalised by Alcaraz and Pimenta to a class of multispin free fermion and free parafermion models [9–11].

Free parafermions are a natural generalisation of the notion of free fermions. In a free fermionic system, the energy eigenvalues are a sum of a set of L fermion quasienergies, each of which is multiplied by a positive or negative sign, giving 2^L combinations for the 2^L eigenvalues of the Hamiltonian. For free parafermions, instead of a positive or negative contribution, each quasienergy is multiplied by an Nth root of unity, i.e., a power of $\omega = \exp(2\pi i/N)$. Thus a general energy eigenvalue is given by

$$E = -\sum_{j=1}^{L} \omega^{q_j} \epsilon_j, \tag{3}$$

where ϵ_j are the parafermion energies or quasienergies, and $q_j \in \{0, \dots, N-1\}$. Each possible combination of q_j values determines a different eigenvalue, giving all N^L states. Figure (1) provides an illustration of such a spectrum.
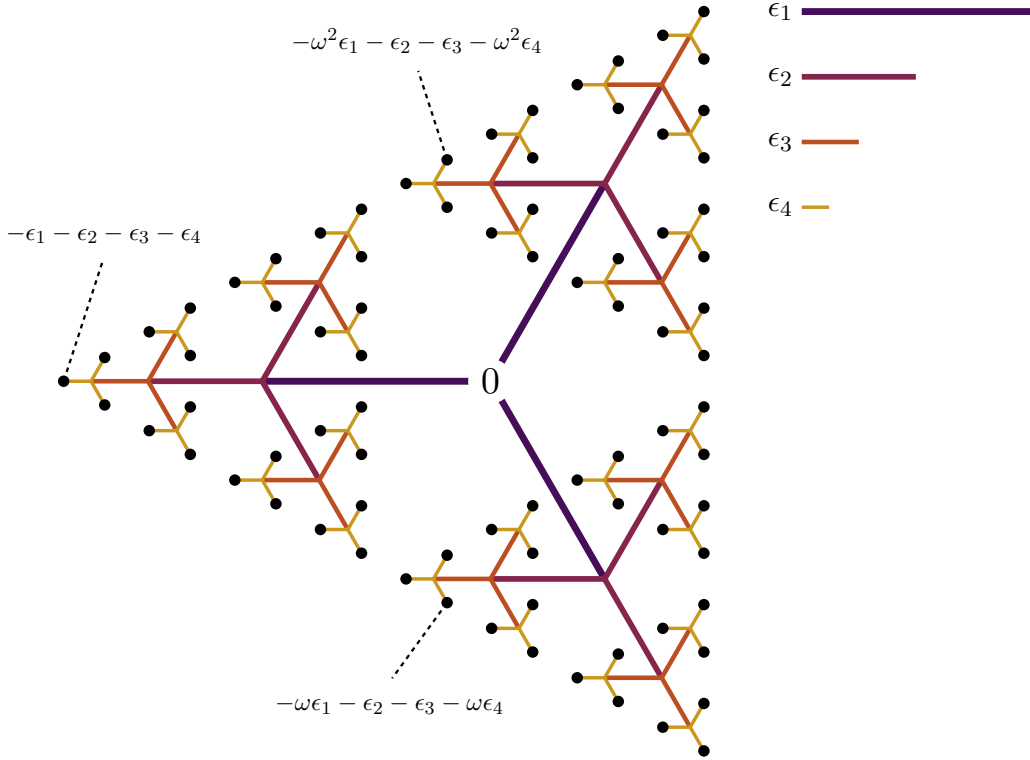
Figure 1: A free parafermion spectrum in the complex plane, for $N = 3$, $L = 4$. The black dots are the N^L energy eigenstates. The spectrum is built up by starting at zero and adding each parafermion multiplied by a power of the root of unity $\omega = \exp(2\pi i/N)$, as per Eq. (3). Here the values of ϵ_j are arbitrary and for most realistic values the paths will overlap each other, but will have the same essential branching structure. Algebraic expressions are shown for some example states, including the ground state $E_0 = -\epsilon_1 - \epsilon_2 - \epsilon_3 - \epsilon_4$.

The quasienergies ϵ_j are real and positive for real and positive λ. They were determined in Baxter's original paper, and in a number of other ways in the literature. Alcaraz et al. [12] calculated them in terms of a quasimomentum variable k:

$$\epsilon_{k_j} = (1 + \lambda^N + 2\lambda^{N/2} \cos k_j)^{1/N}, \tag{4}$$

where k_j are the L solutions of

$$\sin([L+1]k) = -\lambda^{-N/2} \sin(Lk). \tag{5}$$

This formulation is convenient for the analytic approaches used in this work. The quasienergies are equivalently given by the eigenvalues of matrix [13]

$$\mathcal{M} = \begin{pmatrix} 1 & g & & & \\ g & 1+g^2 & g & & \\ & g & 1+g^2 & \ddots & \\ & & \ddots & \ddots & g \\ & & & g & 1+g^2 \end{pmatrix}, \tag{6}$$

where $g = \lambda^{-N/2}$. The parafermions are then $\epsilon_j = \lambda a_j^{1/N}$, where a_j is an eigenvalue of $\mathcal{M}$. Diagonalising $\mathcal{M}$ is an efficient way to find the quasienergies numerically, and is

used to obtain most of the numerical results found in this paper. Alcaraz et al. [12] also determined other quantities including the critical heat exponent, and the ground state energy in the thermodynamic limit:

$$e_\infty(\lambda) = -\,_2F_1\left(-\frac{1}{N}, -\frac{1}{N}; 1; \lambda^N\right), \tag{7}$$

where $_2F_1$ is the hypergeometric function.

In Baxter's paper and in subsequent work, more general models with arbitrary (real and positive) coefficients on each term in Eq. (1) are considered. These have the effect of changing the quasienergies but do not change the free parafermion character of the spectrum. Only uniform models are considered in the present work.

1.1 Periodic Systems and non-Hermitian Physics

The free parafermion model exhibits very different behavior under periodic boundary conditions, which are implemented by adding the boundary term $-Z_L^\dagger Z_1$ to Eq. (1). In fact, the free parafermion solution no longer applies whatsoever, unlike many free fermion systems where the system breaks into free fermionic momentum sectors. Surprisingly, the energy of the system depends on the boundary conditions even in the thermodynamic limit ($L \to \infty$), which is impossible in a Hermitian system [13]. This is an example of a *non-Hermitian skin effect* and has recently been observed in a variety of non-Hermitian systems [14–16].

Recently, there has been extensive activity surrounding non-Hermitian models. Much of their behaviour relates to *exceptional points*, which are degeneracies in the spectrum of a Hamiltonian or other operator where the eigenvectors also coalesce, i.e., two energy eigenvalues become equal, and the corresponding eigenvectors become parallel. This is exclusively a non-Hermitian effect, and for a Hermitian operator all eigenvectors are always orthogonal. The non-Hermitian skin effect, geometric phases, the anomalous bulk-boundary correspondence, and exotic phase transitions may all be related to a system's exceptional points. See Bergholtz et al. [17] for a recent review of these developments, and Ashida et al. [18] for an excellent extensive review of non-Hermitian physics. To our knowledge, no exceptional points have been observed in this Ising spin chain or free parafermion systems.

1.2 Symmetries

The free parafermion model has a $\mathbb{Z}_N$ symmetry generated by the operator $\prod_{j=1}^{L} X_j$, which rotates each clock by one place. It also has parity-time ($\mathcal{PT}$) symmetry, with the action of the operators $\mathcal{P}$ and $\mathcal{T}$ being as follows:

$$\mathcal{P}Z_j\mathcal{P} = Z_{L+1-j} \quad , \quad \mathcal{P}X_j\mathcal{P} = X_{L+1-j}, \tag{8}$$

$$\mathcal{T}Z_j\mathcal{T} = Z_j^\dagger \quad , \quad \mathcal{T}X_j\mathcal{T} = X_j. \tag{9}$$

The parity operator $\mathcal{P}$ inverts or flips the lattice, and the time-reversal operator $\mathcal{T}$ conjugates all numbers. There has been great interest in $\mathcal{PT}$-symmetric non-Hermitian systems, beginning with the work of Bender and Boettcher [19]. These systems, while not Hermitian, have real energy spectra when the $\mathcal{PT}$ symmetry is unbroken. With an appropriate metric they have unitary time evolution [20, 21], even if the symmetry is broken, and thus most of the physics of a standard closed quantum system still applies to them. If the $\mathcal{PT}$ symmetry is broken, the eigenvalues appear in conjugate pairs. In the past two decades, non-Hermitian and particularly $\mathcal{PT}$-symmetric physics has been applied

in a large variety of novel experiments and theoretical work. Many examples of this are covered in the review of Ashida et al. [18].

1.3 Motivation

Our previous work on this model with real λ showed unusual properties such as diverging correlation functions [22]. There was no apparent way to explain this behaviour, which appeared to be characteristic of an exceptional point (EP), because there was no obvious way for an EP to occur. This is the motivation for the present study. In particular, we extend the parameter λ to the complex plane and identify the degenerate EPs in the eigenspectrum.

2 Complex λ

In previous works, the parameter λ is assumed to be real and positive. However, many existing results, including the free parafermion spectrum, can be extended to any complex value of λ. This has interesting consequences: the quasienergies ϵ_j become complex, and exceptional points may be found where two of these quasienergies coincide. The analysis of Baxter, Fendley, and Alcaraz et al. [12] which leads to Eqs. (5) and (7) remains valid for complex λ. Figure (2) provides numerical confirmation of this, and demonstrates the basic effect of complex λ on the spectrum and quasienergies.

We parametrise the argument of complex values of λ with the variable ϕ, as follows:

$$\lambda = |\lambda|e^{2\pi i\phi/N}. \tag{10}$$

Due to the model's $\mathbb{Z}_N$ symmetry, a rotation of greater than $2\pi\phi/N$ is equivalent to $2\pi\phi/N - 2\pi/N$. Therefore the spectrum at $\phi = 1$ is the same as $\phi = 0$. This means that all possible behaviour of the spectrum can be seen in the interval $\phi \in \{0, 1\}$, for any value of N, making ϕ a convenient parametrisation for our purposes.

Complex values of λ can be introduced directly into Eq. (1). However the complex factor could also be applied to the Z term of H, or partially to each term. The difference between these choices is an overall rotation in the complex plane, which has no effect on the location of the EPs and most other physics discussed in this work. However, a particular choice does have the property of preserving the orientation of the spectrum in the complex plane as ϕ changes. This is achieved by applying an overall factor of $\exp(-\pi i\phi/N)$ so that half the rotation is applied to each term.

3 Exceptional Points

For real positive λ, the quasienergies ϵ_j are always positive and distinct. For complex λ, the quasienergies are complex, and a pair of them may become equal at certain values of λ, which depend on L and N. These are exceptional points of the matrix Eq. (6), and, as will be shown, correspond to special EPs of the Hamiltonian. It is important to note the distinction between degeneracies of the ϵ_j, which will be referred to as *quasienergy exceptional points*, and EPs of the full Hamiltonian – the *Hamiltonian exceptional points*. As will be demonstrated, each quasienergy EPs gives rise to many Hamiltonian EPs occurring at once, known as *confluent* exceptional points. The Hamiltonian has other degeneracies, however these are not EPs and do not arise from degeneracies of the quasienergies.
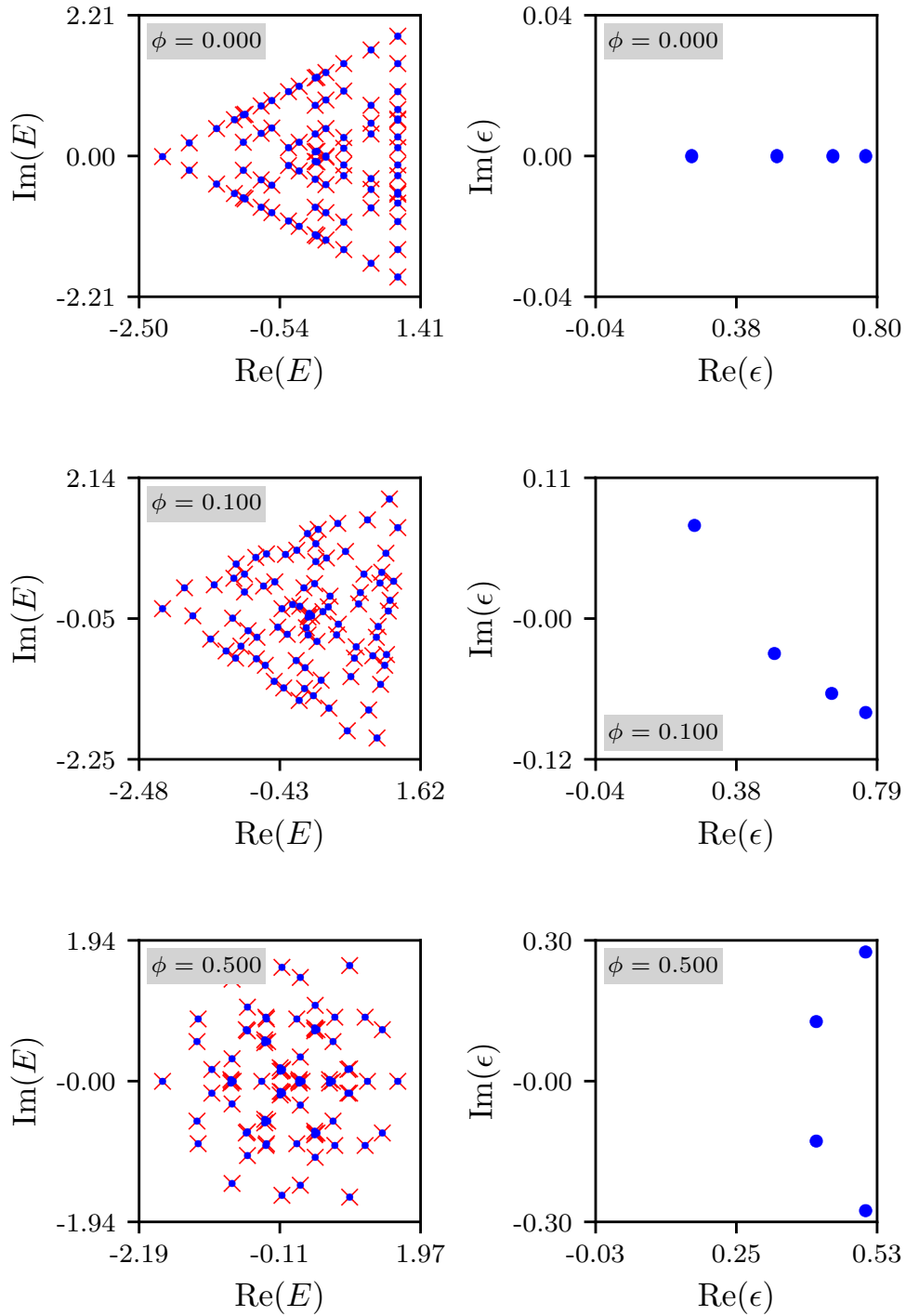
Figure 2: Energy spectra (left) and quasienergies (right) for the free parafermion model with $N = 3$, $L = 4$, $\lambda = 1$ and various values of ϕ. The energies (left) show values obtained from the quasienergies (blue dots), and values obtained from exact diagonalisation of the full Hamiltonian (red crosses). For $\phi = 0.5$ the quasienergies appear in conjugate pairs, restoring the spectrum's $\mathcal{PT}$ symmetry.

A quasienergy EP will occur when Eq. (5) has a repeated root, meaning that both it and its derivative are satisfied:

$$\sin\left([L+1]k\right) + \lambda^{-N/2}\sin(Lk) = 0, \tag{11}$$

and

$$(L+1)\cos\left([L+1]k\right) + L\lambda^{-N/2}\cos(Lk) = 0. \tag{12}$$

The EPs are pairs of values k_{EP} and λ_{EP} which satisfy these equations simultaneously. In other words, the quasienergy EPs occur only at particular values of λ, and at those values they appear as a repeated root k_{EP} of Eq. (5), which gives two degenerate quasienergies. Rearranging the above equation determines k_{EP} as the solution to

$$\sin([2L+1]k) - (2L+1)\sin(k) = 0, \tag{13}$$

with the corresponding value of λ given by

$$\lambda^N = \left[\frac{-\sin([L+1]k)}{\sin(Lk)}\right]^2. \tag{14}$$

In fact, all N complex values of λ that solve Eq. (14) for a given k_{EP} are EPs. These different values occur at rotations of $\exp\left(2\pi i/N\right)$ relative to each other, and have identical spectra. Figure (3) demonstrates how solutions of Eq. (13) appear in the complex plane, and how they correspond to quasienergy degeneracies.

3.1 Hamiltonian Exceptional Points

Is is clear from the form of the energy eigenvalues in Eq. (3) that if two quasienergies are equal ($\epsilon_i = \epsilon_j$) then a macroscopic number N^{L-2} of the eigenvalues of H will also be degenerate in pairs. This does not necessarily mean that these are EPs of the Hamiltonian, where the corresponding eigenvectors coalesce, or alternatively the left and right eigenvectors become orthogonal. However, numerical tests for small L shown in Figure (4) indicate that these quasienergy degeneracies are indeed EPs of H. Similar numerical tests for small L show this to be the case for all the quasienergy EPs identified by Eq. (11), presumably extending to any value of L. There is one exception: the special case $k = 0$, discussed below. Such a coincidence of a macroscopic number of EPs is an unusual phenomenon. The recent work of Znojil [23, 24] suggests that such coincident EPs, referred to as confluent, have special physical properties.

3.2 Trivial Exceptional Points

As mentioned above, there is an exception to the identification of quasienergy degeneracies with Hamiltonian EPs, occurring at $k = n\pi$. In fact, $k = n\pi$ always solves the quasimomentum equation Eq. (5), but Alcaraz et al. [12] and Lieb et al. [25] (in the context of the XY model) only include values of k in the interval $(0, \pi)$, which gives the full set of L associated quasienergies. Therefore it should not be expected that this value is a true EP of the Hamiltonian. Substituting $k = \pi$ into Eq. (12) gives the value

$$\lambda = \left(\frac{L}{L+1}\right)^{N/2}. \tag{15}$$

This point was previously identified [12, 25] as the point where one value of k changes from real and $\leq \pi$, to the form $\pi + iv$ for some $v \in \mathbb{R}$. The corresponding quasienergy
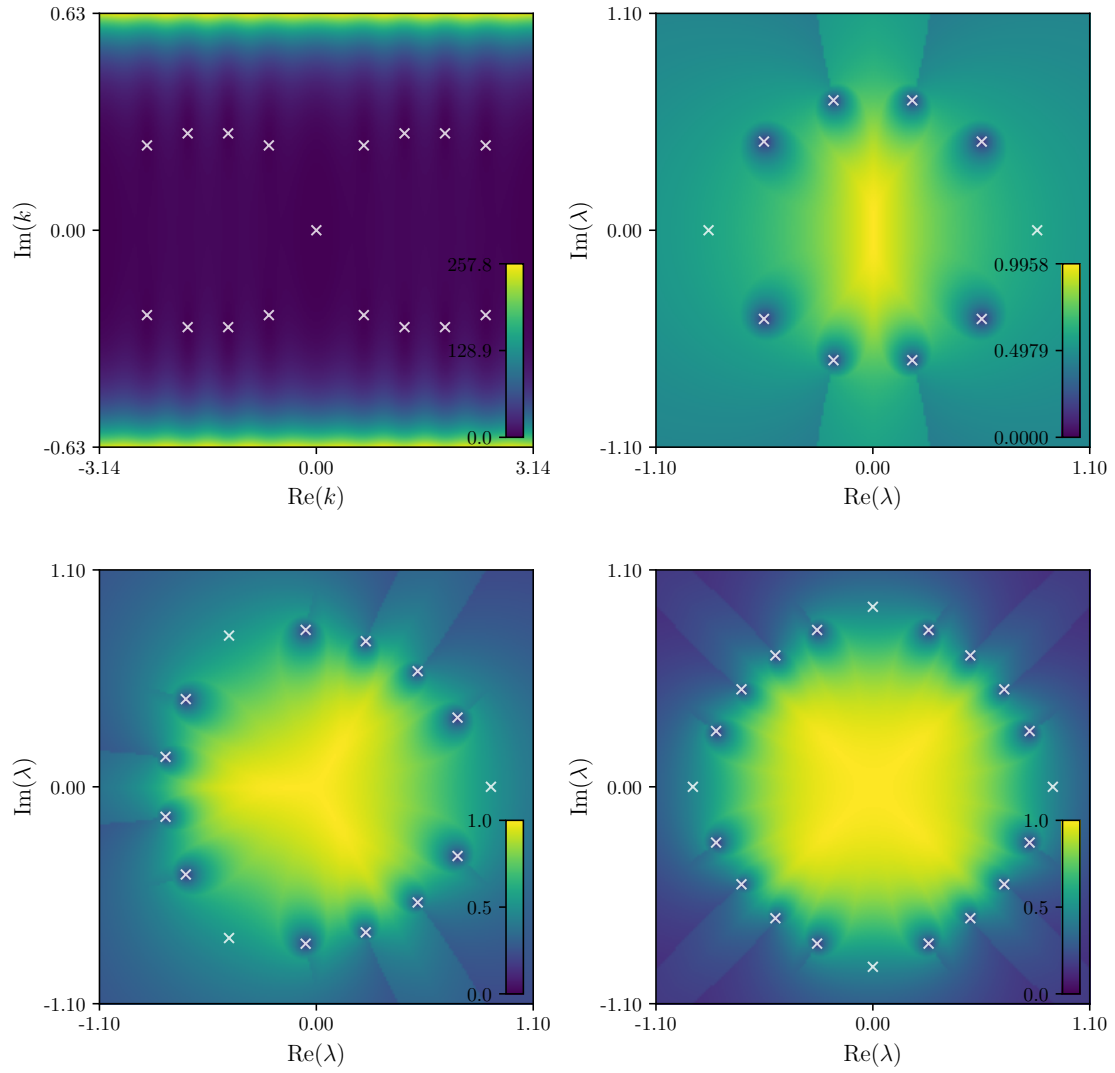
Figure 3: (Top left) Equation (13) evaluated for $L = 4$. The zeros are marked with white crosses. Also shown are the absolute value of the difference between the smallest and second-smallest quasienergies $\Delta\epsilon_{01}$ for $N = 2$ (top right), $N = 3$ (bottom left) and $N = 4$ (bottom right). The zeros from the left subfigure are transformed using Eq. (14) and marked with white crosses in each subfigure. They correspond to actual zeros of $\Delta\epsilon_{01}$ to numerical precision, except for the trivial zero occurring at $k = 0$ and near the roots of unity $\lambda = \exp(2\pi i j/N)$, $j \in \{0, \dots, N-1\}$.

EP
$N = 2$
$L = 4$
$\lambda = 0.6628$
$\phi = 0.2673$

EP, PT-symmetric
$N = 2$
$L = 4$
$\lambda = 0.6439$
$\phi = 0.5000$

EP, trivial
$N = 2$
$L = 4$
$\lambda = 0.8000$
$\phi = 0.0000$

EP
$N = 3$
$L = 3$
$\lambda = 0.7071$
$\phi = 0.3474$
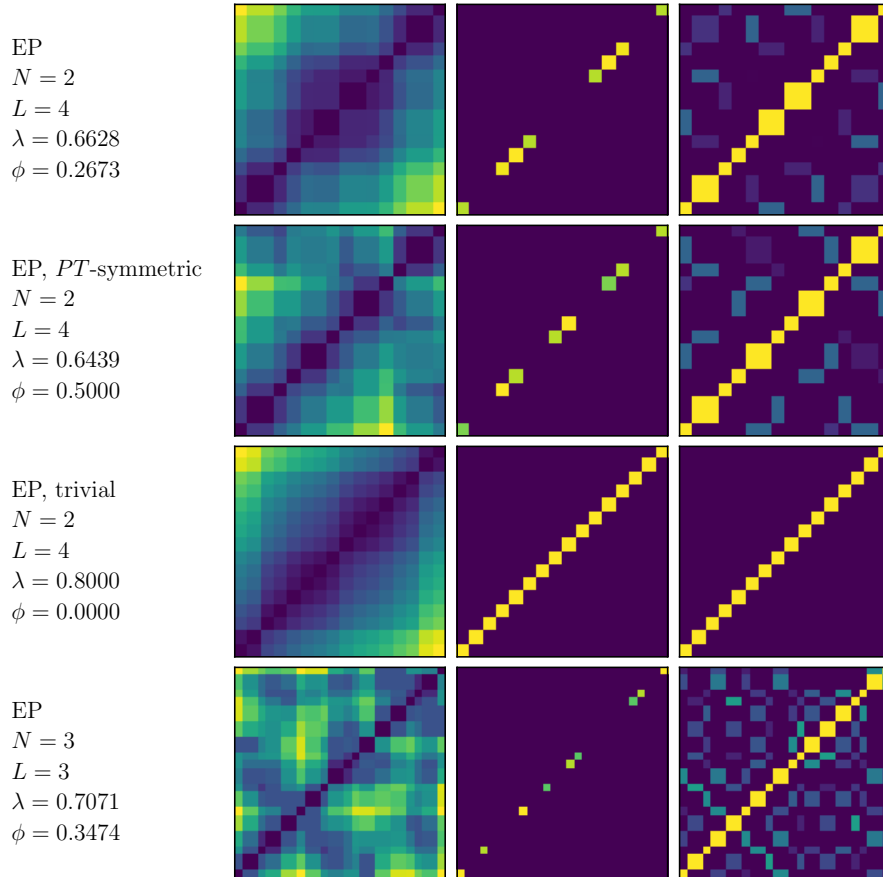
Figure 4: Eigenvector overlap data for the full Hamiltonian at various EPs. All data is scaled from 0 (purple) to 1 (yellow). The x and y axes index the eigenvectors of H, from 1 to N^L. The first column shows the difference between the left and right eigenvalues. The second column shows the overlap of the left and right eigenvectors, with a on-diagonal zero value indicating the left and right eigenvectors becoming orthogonal at an EP. The third column shows the overlap of the right eigenvectors, with an off-diagonal value of 1 indicating the right eigenvectors coalescing at an EP.

approaches 0 as $L \to \infty$, for $\lambda < 1$, which implements unbroken $\mathbb{Z}_N$ symmetry and ground state degeneracy. It may be viewed as a repeated root of Eq. (5), where one root is the trivial root $k = \pi$ which exists for all λ and is not associated with a quasienergy, and another nontrivial root which passes through the point $k = \pi$ while changing from real to complex. Therefore it is not a quasienergy degeneracy in the sense described above, and is not expected to correspond to an EP of H. These trivial EPs are shown in Figs. (3) and (5) alongside the nontrivial EPs.

3.3 A $\mathcal{PT}$-symmetric Exceptional Point

For most values of ϕ, the full Hamiltonian is not $\mathcal{PT}$-symmetric. This makes it unsuitable for interpretation as the Hamiltonian of a closed quantum system. It is $\mathcal{PT}$ symmetric only on the real-λ line, of which only the positive-λ part has been studied in the literature. However, they may occur at the "half-rotated" points, i.e., when $\phi = m + \frac{1}{2}$, where m is an integer. These points do not in all cases have $\mathcal{PT}$ symmetry: although the full spectrum is invariant under PT, the states are permuted and the Hamiltonian does not strictly commute, as λ is conjugated. But for odd N there is one such point that occurs precisely when λ is negative and real. This appears to be the only case where an EP (other than the trivial EPs) occurs where the system is also $\mathcal{PT}$-symmetric.

4 Thermodynamic Limit

The positions of the EPs can be determined in the thermodynamic limit by examining the large-L behaviour of Eq. (13). Following Alcaraz et al. [12] and Lieb et al. [25], k_j may be expanded as

$$k_j = \frac{\pi j}{L} + \frac{a}{L} + \mathcal{O}\left(\frac{1}{L^2}\right), \tag{16}$$

where $j \in \{1 \cdots, L\}$, and a is determined by inserting the expansion into Eq. (11):

$$\cot(\pi a) = -\frac{\lambda^{-N/2} + \cos(\pi j/L)}{\sin(\pi j/L)}. \tag{17}$$

It is worth noting that in Eq. (16), the first term is of order zero since j is of order L. The EPs are given by values of λ and k which satisfy both Eq. (11) and its derivative Eq. (12), which gives a second equation for a at the EPs:

$$\tan(\pi a) = \frac{\frac{L}{L+1}\lambda^{-N/2} + \cos(\pi j/L)}{\sin(\pi j/L)}. \tag{18}$$

Combining the two and setting $L/(L+1) \approx 1$ gives

$$\frac{-\sin(\pi j/L)}{\cos(\pi j/L) + \lambda^{N/2}} = \frac{\cos(\pi j/L) + \lambda^{N/2}}{\sin(\pi j/L)}, \tag{19}$$

which by eliminating a reduces to

$$0 = 1 + 2\lambda^{N/2}\cos\left(\frac{\pi j}{L}\right) + \lambda^N, \tag{20}$$

This has solutions
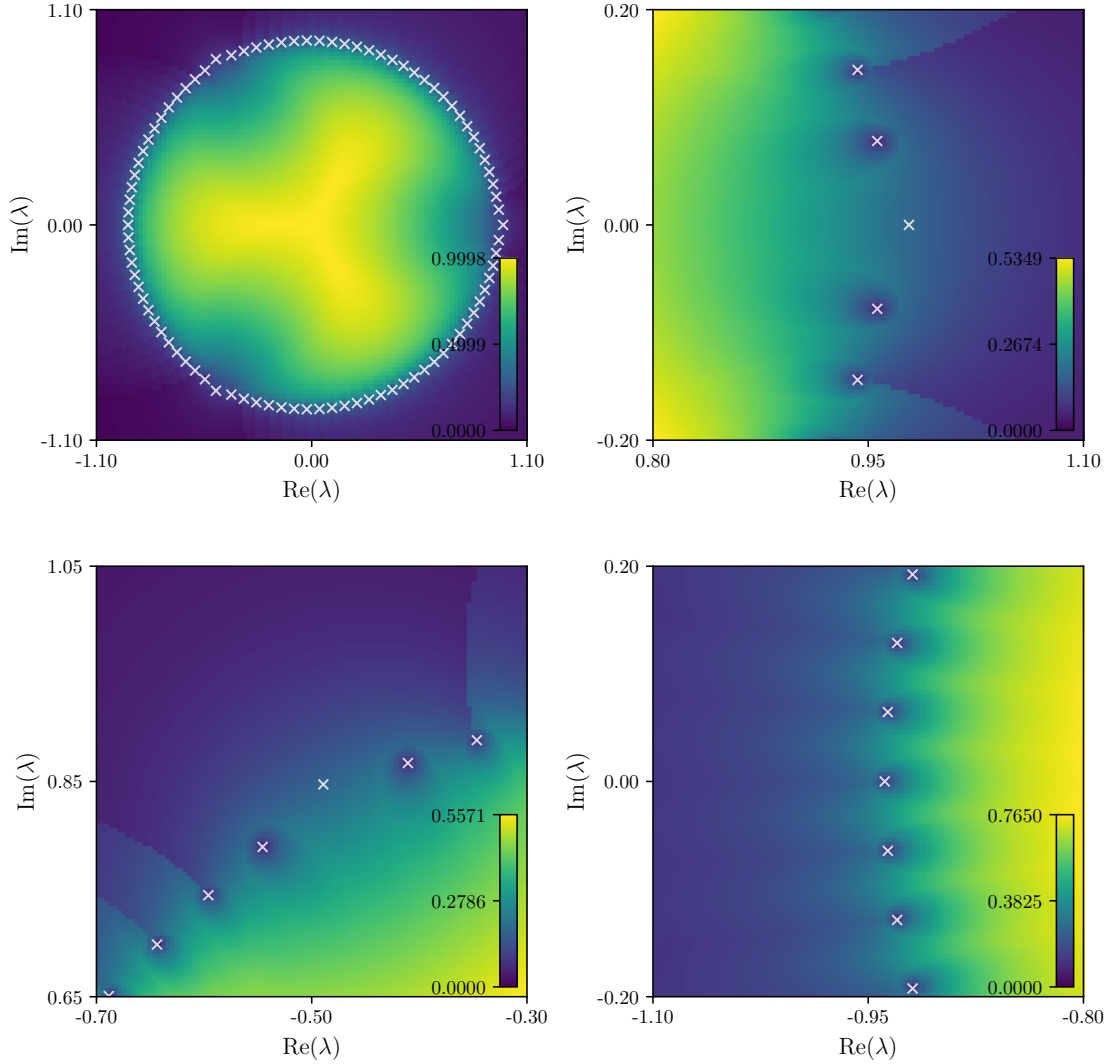
Figure 5: The absolute distance between the smallest two quasienergies for $L = 50$, $N = 3$. The exceptional points found by minimising Eq. (13) are marked with white crosses. Subfigures show different parameter ranges.

$$\lambda^{N/2} = -\cos\left(\frac{\pi j}{L}\right) \pm i\sin\left(\frac{\pi j}{L}\right),\tag{21}$$

which squares to (using double-angle formulae)

$$\lambda^{N} = \cos\left(\frac{2\pi j}{L}\right) \pm i\sin\left(\frac{2\pi j}{L}\right),\tag{22}$$

where $j \in \{1,\dots,L\}$ as defined above. These are precisely the Lth roots of unity, with $j = L$ giving unity, and with each root appearing twice. This repetition results from the fact that for any k defining an EP, or generally a quasienergy satisfying Eq. (11), the conjugate k^* will give the same energy. Taking all solutions for λ, this gives the NL roots of unity which appear to be the limiting case of the data in Fig. (5).

5 Other Degeneracies of H

Degeneracies in the quasienergies have been shown to give rise to confluent EPs of H. However it is possible that H has other EPs. In Fig. (6) the minimal distance between any two eigenvalues of H, $\Delta_{E_{01}}$, is plotted. This function has many zeros even for the small value of $L = 4$. For higher L there would be exponentially more. In principle, these zeros could be EPs of H, or they could be degeneracies of the kind found in Hermitian systems, which do not have orthogonal left and right eigenvectors. Figure (6) provides numerical evidence that most degeneracies of H are not in fact EPs. Subfigures (b), (c), and (d) show various quantities along the real-λ line (for negative values), which includes a quasienergy EP at around $\lambda = -0.75$. Although there are many degeneracies of H along this line (seen in subfigures (a) and (b)), only the degeneracy at the quasienergy EP gives rise to orthogonal left and right eigenvectors, as seen in subfigure (d). Similar numerical tests have been performed for other small values of L and N and show the same behaviour. This suggests that the only EPs of H are the quasienergy EPs, but obviously does not provide conclusive proof.

More generally, if the quasienergies are distinct then a degeneracy of H will occur if some combination of the quasienergies sums to zero when multiplied by appropriate powers of ω, as is clear from the form of the spectrum in Eq. (3), i.e.,

$$\omega^{k_1}\epsilon_{j_1} + \omega^{k_2}\epsilon_{j_2} + \cdots + \omega^{k_m}\epsilon_{j_m} = 0 \tag{23}$$

for some $m \leq L$. Note that this is much more general than the quasienergy EP condition $\epsilon_i - \epsilon_j = 0$. The simplest case of Eq. (23) is one involving only two quasienergies:

$$\omega^k\epsilon_i + \epsilon_j = 0, \tag{24}$$

for some i, j, and k, where the second power of ω has been divided out. Figure (6) suggests that such points are not EPs but merely degeneracies of H (except in cases where $\omega^k = -1$). Further numerical tests, including specifically searching for points satisfying Eq. (24) also indicate that such points are degeneracies of H but not EPs. It may be possible to evaluate simple conditions like Eq. (24) to find degeneracies analytically, however they will not satisfy the condition of repeated roots in Eq. (12) which allowed the determination of the quasienergy EPs. Determining such degeneracies, and the question of whether they can be EPs of H, is a topic for future work.

6 Exceptional Points and Positive Real λ

According to equation (14), there is never an EP for positive real λ. However, the influence of the EPs may still be felt. Tzeng et al. [26,27] describe how EPs in non-Hermitian systems can be detected precisely from numerical data by computing the fidelity susceptibility. They define a generalised fidelity for non-Hermitian systems as

$$\mathcal{F} = \langle L(\lambda)|R(\lambda + \delta)\rangle\langle(\lambda + \delta)|R(\lambda)\rangle, \tag{25}$$

where δ is a small parameter, and $\langle L|$ and $|R\rangle$ are the left and right ground states (or any state of interest). The fidelity susceptibility χ is the second-order expansion coefficient in δ, which is approximately

$$\chi \approx \frac{1 - \mathcal{F}}{\delta^2}. \tag{26}$$
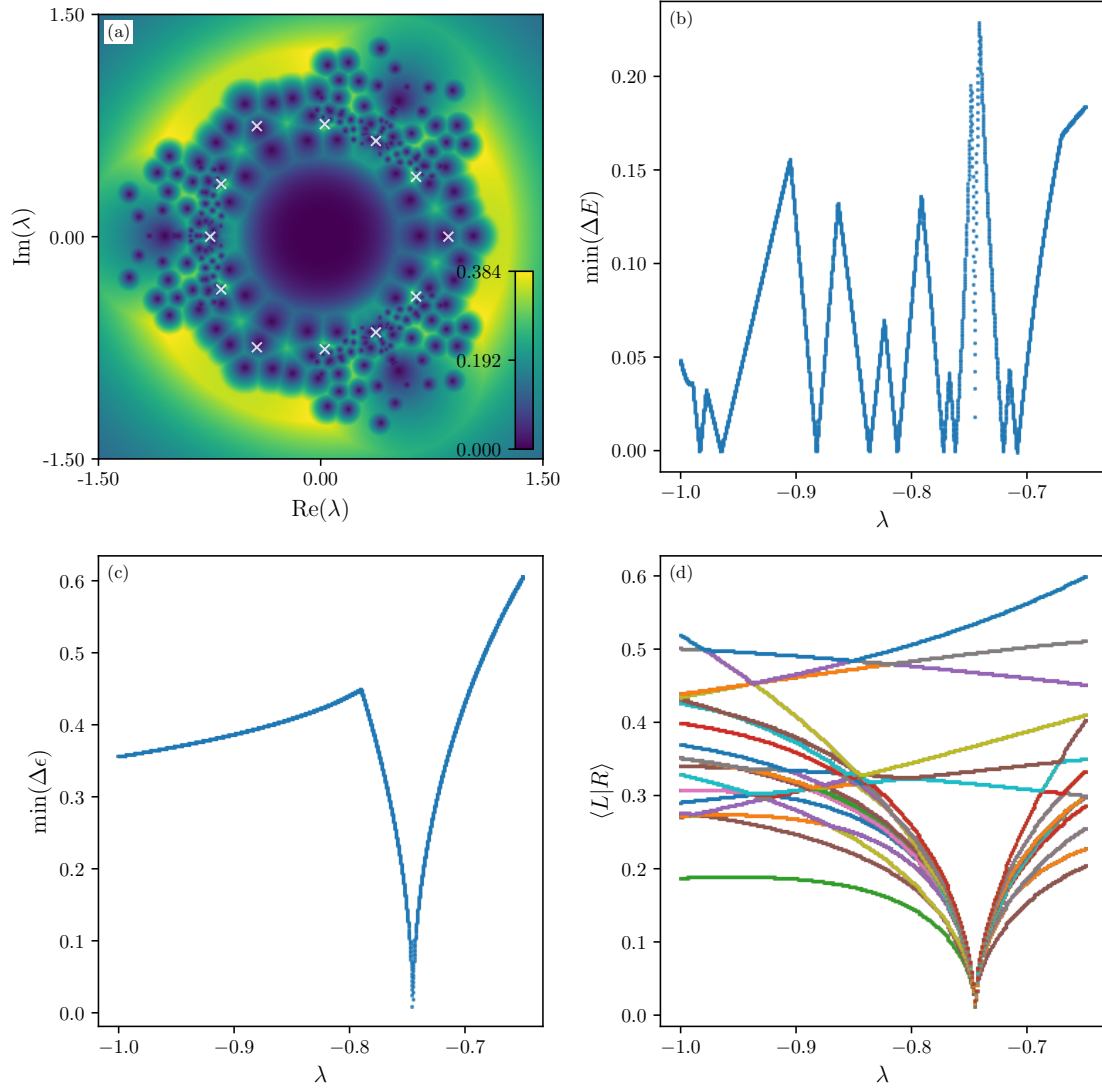
Figure 6: For $N = 3$, $L = 4$, (a) Smallest distance between any two eigenvalues of the Hamiltonian $\Delta_{E_{01}}$. The EPs obtained from Eq. (14) are marked with white crosses. Although not clearly visible, these quasienergy EPs correspond to zeros of $\Delta_{E_{01}}$, as they must given the free parafermion spectrum. (b) Smallest distance between any two eigenvalues for negative real λ. (c) Smallest distance between quasienergies for negative real λ. (d) Overlaps of the left and right eigenvectors of the Hamiltonian for negative real λ.

At or nearby a critical point, $\text{Re}(\chi) \to +\infty$, while at an EP $\text{Re}(\chi) \to -\infty$. Although no EPs exist for positive real λ, the EPs near the unit circle come arbitrary close to this line as L increases. This produces a strong effect in the fidelity susceptibility.

Figure (7) shows fidelity susceptibility data for the free parafermion model obtained using the density matrix renormalisation group method. A value of $\delta = 10^{-5}$ is used for the expansion parameter. This data is for moderate system sizes with $N = 2$ and $N = 3$, with real and positive values of λ which are not expected to exhibit EPs. Nonetheless, for $N = 3$ characteristic EP behaviour is observed near $\lambda = 1$. Since the $N = 2$ Ising case is Hermitian for real λ, it is impossible for this behaviour to occur despite the proximity of the EPs. This can potentially be explained by the contributions from the proximate EPs cancelling out for $N = 2$ but not $N = 3$, but requires further investigation. The left-right ground state overlap is also shown for $N = 3$, demonstrating that the left and right eigenvectors approach orthogonality.
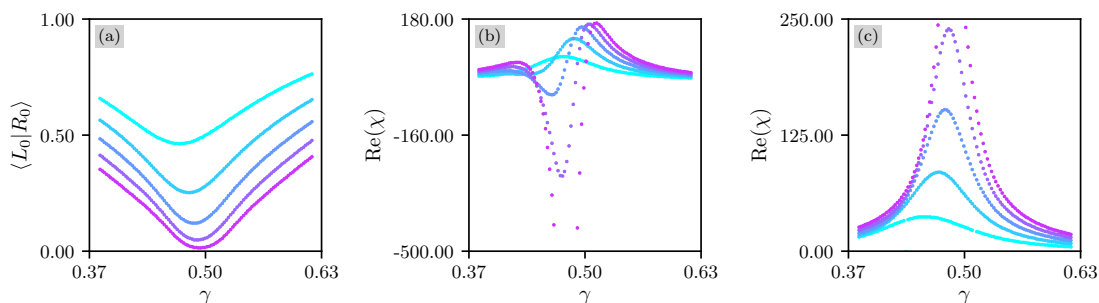
Figure 7: Overlap and fidelity susceptibility for $L = 10$ (cyan), 15, 20, 25, 30 (purple). (a) Left-right ground state overlap for $N = 3$. (b) Fidelity susceptibility for $N = 3$. (c) Fidelity susceptibility for $N = 2$. γ is a rescaled analog of λ, with $\lambda = \frac{\gamma+1}{\gamma}$. The critical point is at $\gamma = 0.5$.

7 Conclusion

Our previous work [22] on the Baxter-Fendley free parafermion model with positive real λ showed unusual diverging correlation functions which are characteristic of the presence of an exceptional point. However, such a point is unlikely for real positive λ given the distinctness of the quasienergies. Inspired by this, we have extended λ to the complex plane, which reveals a set of NL EPs which approach the unit circle in the thermodynamic limit. This means that as $L \to \infty$, the EPs come arbitrarily close to the real positive λ axis. This explains how behaviour like diverging correlation functions could occur. The details of these divergences near the EPs is a topic for further consideration. These exceptional points derive from degeneracies of the quasienergies which define the model's free spectrum, and each quasienergy degeneracy corresponds to a macroscopic number of coincident or confluent EPs of the Hamiltonian. We have derived an analytic expression which identifies these points, Eq. (13).

The EPs also exist in the familiar Ising spin chain, which is the limiting case ($N = 2$) of the free parafermion model. They do not produce unusual behaviour on the real axis in this case, as the model is Hermitian for real λ. However the existence of these points appears to be unexplored in the literature, despite the fact that the Ising chain has been

studied very extensively. The behaviour of the EPs resembles Lee-Yang zeros [28], in that they appear on the unit circle, they appear as a consequence of making the model parameter complex, and they approach the critical point as $L \to \infty$.

Acknowledgements

Some of the numerical calculations (DMRG and exact diagonalisation) were performed using the excellent TeNPy Library [29]. RAH thanks the staff of the National Computational Infrastructure facility at ANU for their generous advice and other assistance.

Funding information This work has been supported by the Australian Research Council through grant number DP210102243.

References

[1] R. J. Baxter, *A simple solvable Z(N) Hamiltonian*, Physics Letters A **140**(4), 155 (1989), doi:10.1016/0375-9601(89)90884-0.

[2] R. J. Baxter, *Superintegrable chiral Potts model: Thermodynamic properties, an "inverse" model, and a simple associated Hamiltonian*, Journal of Statistical Physics **57**(1-2), 1 (1989), doi:10.1007/BF01023632.

[3] P. Fendley, *Free parafermions*, Journal of Physics A: Mathematical and Theoretical **47**(7), 075001 (2014), doi:10.1088/1751-8113/47/7/075001.

[4] R. J. Baxter, *The tau-2 model and parafermions*, Journal of Physics A: Mathematical and Theoretical **47**(31), 315001 (2014), doi:10.1088/1751-8113/47/31/315001.

[5] H. Au-Yang and J. H. H. Perk, *Parafermions in the tau-2 model*, Journal of Physics A: Mathematical and Theoretical **47**(31), 315002 (2014), doi:10.1088/1751-8113/47/31/315002.

[6] H. Au-Yang and J. H. H. Perk, *Parafermions in the tau-2 model II*, arXiv:1606.06319 [math-ph] (2016), `1606.06319`.

[7] V. V. Bazhanov and Y. G. Stroganov, *Chiral Potts model as a descendant of the six-vertex model*, Journal of Statistical Physics **59**(3), 799 (1990).

[8] P. Fendley, *Free fermions in disguise*, Journal of Physics A: Mathematical and Theoretical **52**(33), 335002 (2019), doi:10.1088/1751-8121/ab305d.

[9] F. C. Alcaraz and R. A. Pimenta, *Integrable quantum spin chains with free fermionic and parafermionic spectrum*, Physical Review B **102**(23), 235170 (2020), doi:10.1103/PhysRevB.102.235170.

[10] F. C. Alcaraz and R. A. Pimenta, *Free fermionic and parafermionic quantum spin chains with multispin interactions*, Physical Review B **102**(12), 121101 (2020), doi:10.1103/PhysRevB.102.121101.

[11] F. C. Alcaraz and R. A. Pimenta, *Free-parafermionic Z(N) and free-fermionic XY quantum chains*, Physical Review E **104**(5), 054121 (2021), doi:10.1103/PhysRevE.104.054121.

[12] F. C. Alcaraz, M. T. Batchelor and Z.-Z. Liu, *Energy spectrum and critical exponents of the free parafermion Z(N) spin chain*, Journal of Physics A: Mathematical and Theoretical **50**(16), 16LT03 (2017), doi:10.1088/1751-8121/aa645a, `1612.02617`.

[13] F. C. Alcaraz and M. T. Batchelor, *Anomalous bulk behaviour in the free parafermion Z(N) spin chain*, arXiv:1802.04453 [cond-mat, physics:hep-th, physics:math-ph, physics:quant-ph] (2018), `1802.04453`.

[14] F. Song, S. Yao and Z. Wang, *Non-Hermitian Skin Effect and Chiral Damping in Open Quantum Systems*, Physical Review Letters **123**(17), 170401 (2019), doi:10.1103/PhysRevLett.123.170401.

[15] L. Li, C. H. Lee, S. Mu and J. Gong, *Critical non-Hermitian skin effect*, Nature Communications **11**(1), 5491 (2020), doi:10.1038/s41467-020-18917-4.

[16] K. Kawabata, M. Sato and K. Shiozaki, *Higher-order non-Hermitian skin effect*, Physical Review B **102**(20), 205118 (2020), doi:10.1103/PhysRevB.102.205118.

[17] E. J. Bergholtz, J. C. Budich and F. K. Kunst, *Exceptional topology of non-Hermitian systems*, Reviews of Modern Physics **93**(1), 015005 (2021), doi:10.1103/RevModPhys.93.015005.

[18] Y. Ashida, Z. Gong and M. Ueda, *Non-Hermitian Physics*, Advances in Physics **69**(3), 249 (2020), doi:10.1080/00018732.2021.1876991, `2006.01837`.

[19] C. M. Bender and S. Boettcher, *Real Spectra in Non-Hermitian Hamiltonians Having PT Symmetry*, Physical Review Letters **80**(24), 5243 (1998), doi:10.1103/PhysRevLett.80.5243.

[20] P. D. Mannheim, *PT symmetry as a necessary and sufficient condition for unitary time evolution*, Philosophical Transactions of the Royal Society A: Mathematical, Physical and Engineering Sciences **371**(1989), 20120060 (2013).

[21] C. M. Bender, S. Boettcher and P. N. Meisinger, *PT-symmetric quantum mechanics*, Journal of Mathematical Physics **40**(5), 2201 (1999), doi:10.1063/1.532860.

[22] Z.-Z. Liu, R. A. Henry, M. T. Batchelor and H.-Q. Zhou, *Some ground-state expectation values for the free parafermion Z(N) spin chain*, Journal of Statistical Mechanics: Theory and Experiment **2019**(12), 124002 (2019), doi:10.1088/1742-5468/ab4fe1.

[23] M. Znojil, *Passage through exceptional point: Case study*, Proceedings of the Royal Society A: Mathematical, Physical and Engineering Sciences **476**(2236), 20190831 (2020), doi:10.1098/rspa.2019.0831.

[24] M. Znojil, *Confluences of exceptional points and a systematic classification of quantum catastrophes*, Scientific Reports **12**(1), 3355 (2022), doi:10.1038/s41598-022-07345-7.

[25] E. Lieb, T. Schultz and D. Mattis, *Two soluble models of an antiferromagnetic chain*, Annals of Physics **16**(3), 407 (1961), doi:10.1016/0003-4916(61)90115-4.

[26] Y.-C. Tzeng, C.-Y. Ju, G.-Y. Chen and W.-M. Huang, *Hunting for the non-Hermitian exceptional points with fidelity susceptibility*, Physical Review Research **3**(1), 013015 (2021), doi:10.1103/PhysRevResearch.3.013015.

[27] Y.-T. Tu, I. Jang, P.-Y. Chang and Y.-C. Tzeng, *General properties of fidelity in non-Hermitian quantum systems with PT symmetry*, arXiv:2203.01834 [cond-mat, physics:physics, physics:quant-ph] (2022), `2203.01834`.

[28] T. D. Lee and C. N. Yang, *Statistical Theory of Equations of State and Phase Transitions. II. Lattice Gas and Ising Model*, Physical Review **87**(3), 410 (1952), doi:10.1103/PhysRev.87.410.

[29] J. Hauschild and F. Pollmann, *Efficient numerical simulations with Tensor Networks: Tensor Network Python (TeNPy)*, SciPost Phys. Lect. Notes p. 5 (2018), doi:10.21468/SciPostPhysLectNotes.5.